The Journal of Experimental Biology 206, 233-243

doi:10.1242/jeb.00066

The dependence of electrical transport pathways in Malpighian tubules on ATP

Daniel S. Wu and Klaus W. Beyenbach*

Department of Biomedical Sciences, VRT 8014, Cornell University, Ithaca, NY 14853, USA

*Author for correspondence (e-mail: kwb1@cornell.edu)

Accepted 10 October 2002

Summary

The relationship between the intracellular ATP concentration $[ATP]_i$ and the electrical properties of principal cells was investigated in Malpighian tubules of the yellow fever mosquito, *Aedes aegypti*. Under control conditions, $[ATP]_i$ was 0.91 mmol l^{-1}, the input resistance of the principal cell (R_{pc}) was 334.1 kΩ, and the basolateral membrane was marked by a large K^+-conductance and a membrane voltage (V_{bl}) of –75.8 mV. Peritubular cyanide (CN, 0.3 mmol l^{-1}) reduced $[ATP]_i$ to 0.08 mmol l^{-1} in less than 2 min; however, V_{bl} dropped to –8 mV and R_{pc} increased to 3150.8 kΩ in 8 min, while the K^+-conductance of the basolateral membrane disappeared. Upon washout of CN, V_{bl} and R_{pc} returned to control values within 2 min, and the basolateral membrane recovered its K^+-conductance. The recovery of normal $[ATP]_i$ took 15 min. Dose-dependence and EC_{50} values for the CN-inhibition of V_{bl} and the increase in R_{pc} were strikingly similar (184.0 μmol l^{-1} and 164.4 μmol l^{-1}). Similar effects of metabolic inhibition were observed with dinitrophenol (DNP), but the EC_{50} values were 50.3 μmol l^{-1} and 71.7 μmol l^{-1} for the effects on V_{bl} and R_{pc}, respectively. Barium, a blocker of K^+-channels, significantly hyperpolarized V_{bl} to –89.1 mV and increased R_{pc} to 769.4 kΩ under control conditions, but had no effects during metabolic inhibition. These results illustrate a temporal relationship between $[ATP]_i$ and electrogenic and conductive transport pathways in principal cells that is consistent with the role of ATP as an integrator of transport steps at apical and basolateral membranes of the cell. When $[ATP]_i$ drops to levels that are 10% of control, the V-type H^+-ATPase is inhibited, preventing the extrusion of K^+ to the tubule lumen. At the same time, basolateral membrane K^+-channels close, preventing the entry of K^+ from the hemolymph. Intracellular K^+ homeostasis is thus protected during metabolic inhibition, allowing the cell to re-establish K^+ transport when ATP is synthesized again.

Key words: Malphigian tubule, ATP, yellow fever mosquito, *Aedes aegypti*, metabolism, electrogenic transport, electroconductive transport.

Introduction

Studies of transepithelial transport typically focus on the movement of ions, organic solutes and water across the epithelium, but what drives transport is ultimately metabolism. The latter has not received much attention in studies of epithelial transport. However, metabolism and transepithelial transport must be intimately coupled, especially in actively transporting epithelia, such as Malpighian tubules. Indeed, in Malpighian tubules of the yellow fever mosquito *Aedes aegypti*, the inhibition of oxidative phosphorylation with dinitrophenol brings transepithelial electrolyte and water secretion immediately to a halt and eliminates voltages across cell membranes and the whole epithelium (Beyenbach, 2001).

Since the product of oxidative phosphorylation is ATP, the present study was undertaken to examine the relationship between intracellular ATP concentration ($[ATP]_i$) and electroconductive and electrogenic transport mechanisms in principal cells of Malpighian tubules of the yellow fever mosquito. Principal cells are the sites of Na^+ and K^+ secretion from the hemolymph into the tubule lumen (Beyenbach, 1995). The entry of K^+ into the cell from the hemolymph is electroconductive through K^+-channels in the basolateral membrane (Fig. 1). On the apical side of the cell, extrusion of K^+ from the cytoplasm into the tubule lumen is thought to be mediated by an nH^+/K^+ exchanger that, in turn, is driven by the electrochemical H^+ potential generated across the membrane by the activity of the electrogenic V-type H^+-ATPase, also located in the apical membrane. To examine the relationship between $[ATP]_i$ and electroconductive and electrogenic transport mechanisms in principal cells of the tubule, we measured the effects of metabolic inhibition on $[ATP]_i$ in one set of tubules, and the effects on membrane voltage and resistance of principal cells in another set of tubules. We found that a severe reduction in $[ATP]_i$ not only inhibited the electrogenic V-type H^+-ATPase at the apical membrane but also blocked the K^+-conductance of the basolateral membrane at the same time. Simultaneous changes at both apical and basolateral membranes as a function of $[ATP]_i$ suggest that ATP integrates the transport steps at these two cell membranes. In the absence of ATP synthesis, the drop of $[ATP]_i$ to 10% of control levels effectively isolates the cell

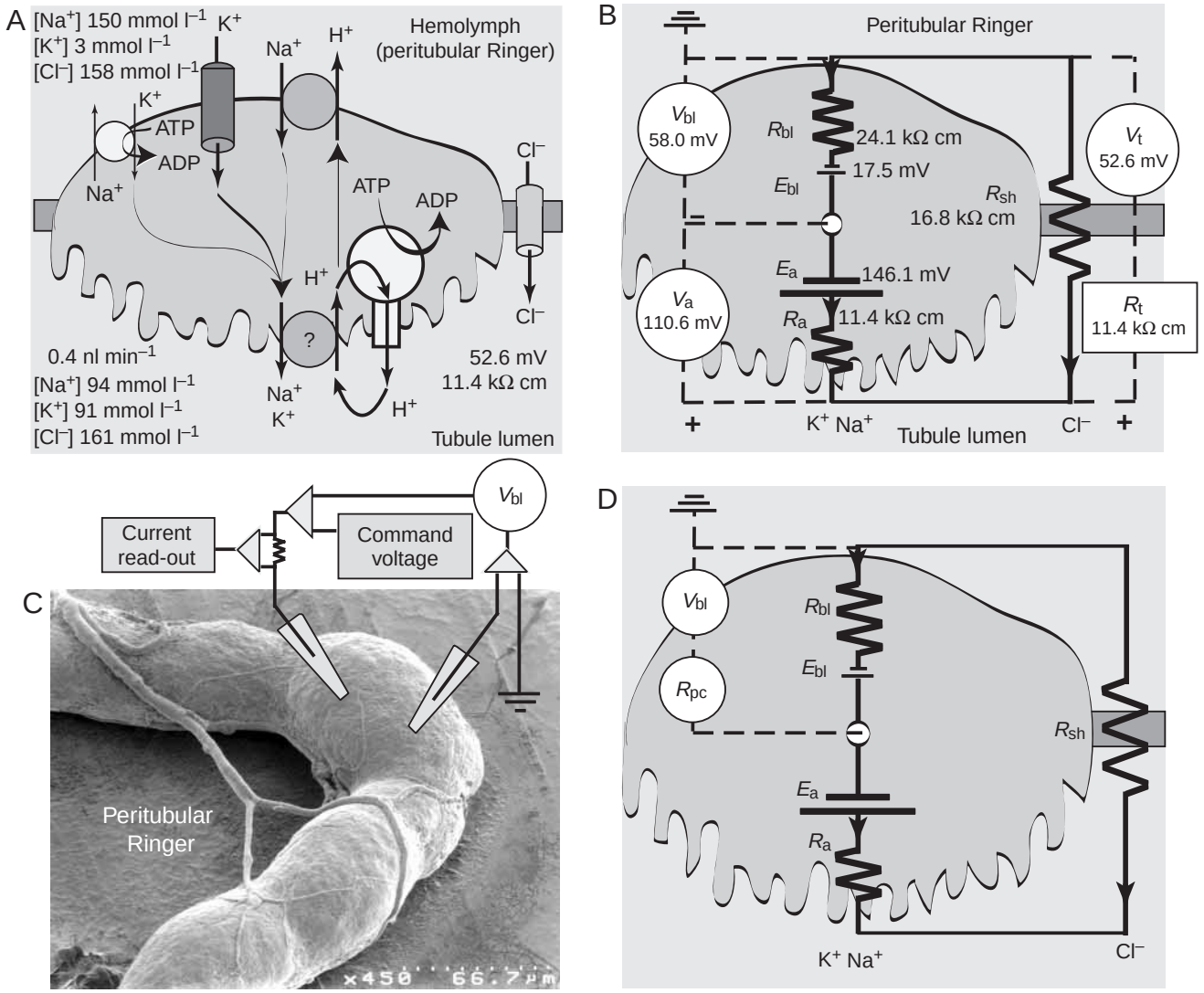

Fig. 1. Electrophysiological study of a principal cell by the two-electrode voltage-clamp (TEVC) method in isolated Malpighian tubules of *Aedes aegypti*. (A) Transepithelial secretion of NaCl and KCl under control conditions. The question mark indicates uncertainty as to whether the exchanger transports both Na^+ and K^+. (B) Electrical equivalent circuit of transepithelial NaCl and KCl secretion consisting of the active transport pathway for Na^+ and K^+ ions through principal cells and the passive transport of Cl^- through the shunt pathway. E_{bl} and E_a are the electromotive forces at the basolateral and apical membrane, respectively. R_{bl}, R_a and R_{sh} are the resistances of the basolateral membrane, the apical membrane, and the shunt, respectively. V is voltage measured across basolateral (bl) and apical (a) membranes of the cell. V_t and R_t are the transepithelial voltage (lumen-positive) and resistance, respectively. Numerical data are from previous studies (Pannabecker et al., 1992). (C) TEVC study of a principal cell in an isolated Malpighian tubule. (D) The measurement circuit in TEVC studies yields the input resistance R_{pc}, which is the sum of the parallel resistances of the basolateral membrane and the apical membrane in series with the shunt.

from its luminal and peritubular environment, apparently preserving intracellular homeostasis that allows electrogenic and electroconductive transport mechanisms to spring back again when ATP can be synthesized again.

Materials and methods

Mosquitoes and Malpighian tubules

The colony of yellow fever mosquitoes *Aedes aegypti* L. was maintained as described previously (Pannabecker et al., 1993). On the day of the experiment, a female mosquito, aged 3–7 days post-eclosion, was cold-anesthetized and decapitated. A light tug on the posterior abdomen freed the gastrointestinal tract and the five Malpighian tubules from the abdominal cavity. A Malpighian tubule was removed from its attachment at the junction of mid- and hindgut and transferred to a Lucite perfusion bath with a filling volume of 500 µl. The bottom of the bath had a coat of black dissecting wax to which Malpighian tubules would adhere, stabilizing the tubule for microelectrode recordings from its principal cells. The tubules were viewed from above through a stereo microscope at 50× magnification (Wild, Heerbrugg, Switzerland).

Ringer solution and inhibitors

The control Ringer solution consisted of the following solutes, in mmol l^{-1}: 150.0 NaCl, 25.0 Hepes, 3.4 KCl, 1.8 $NaHCO_3$, 1.0 $MgCl_2$, 1.7 $CaCl_2$ and 5.0 glucose. The pH was adjusted to 7.1 with 1 mol l^{-1} NaOH. The osmolality of the Ringer solution was 320 mosmol kg^{-1} H_2O. High K^+ solutions contained 34 mmol l^{-1} KCl, where K^+ replaced Na^+ in equimolar quantities. $BaCl_2$, a K^+-channel blocker, was used at a concentration of 5 mmol l^{-1} and, to balance osmolarity, 15 mmol l^{-1} mannitol was added to the control Ringer solution. To inhibit ATP synthesis we used dinitrophenol (DNP, Sigma) or KCN (CN, Fisher Scientific) at 0.1 mmol l^{-1} and 0.3 mmol l^{-1}, respectively. Control or test Ringer solutions continuously flowed through the Lucite perfusion bath at a rate of 2.4 ml min^{-1}. The actual bath volume was adjusted to approximately 250 µl by positioning the height of the suction outflow line. Accordingly, the half-time for changing the bath was approximately 4.3 s, on the assumption that the bath change obeyed first-order kinetics. The bath was considered completely exchanged after 10 half-times, i.e. 43 s.

Intracellular ATP concentrations

We used the luciferin/luciferase method to measure ATP concentrations, using the Calbiochem kit no. 119108, (La Jolla, CA, USA). Luminescence was measured with the Lumat B9501 luminometer (Berthold Australia Pty Ltd, Bundoora, Australia). Relative light units (RLU) of unknown quantities of ATP were read against those of known quantities of ATP (Calbiochem) and corrected for the background luminescence of a blank, consisting of 100 µl Ringer solution plus 100 µl releasing reagent (Calbiochem kit). A double-log plot of moles of ATP *versus* RLU yielded linear standard curves with regression coefficients >0.99. Exploratory ATP assays in Malpighian tubules advised the use of ATP standards ranging between 10^{-9} to 10^{-11} moles to bracket the ATP content of five Malpighian tubules.

The ATP content was routinely measured in the complete set of five Malpighian tubules isolated from a single adult female mosquito. After depositing the five tubules in 500 µl Ringer solution, 500 µl of ATP- releasing reagent (Calbiochem) was added and stirred with a Vortex mixer for 10 s. To a 200 µl sample of this tubule extract, 100 µl of luciferin/luciferase was added and immediately read in the luminometer. The average RLU was taken from three replicates. After regression of RLU to ATP concentration, the average $[ATP]_i$ was estimated from the average dimension of the female *Aedes* Malpighian tubule (length, 3.5 mm; o.d., 100 µm, i.d. 10 µm).

To observe how rapidly $[ATP]_i$ would drop after metabolic inhibition with cyanide or dinitrophenol, we added 50 µl of 3 mmol l^{-1} KCN or 1 mmol l^{-1} DNP to a set of five Malpighian tubules at time zero and measured $[ATP]_i$ between 15 s to 8 min later. To measure the recovery of ATP concentrations after treatment with CN, tubules were exposed to 0.3 mmol l^{-1} CN for 8 min. CN was then washed out and ATP concentrations were measured 1–18 min later.

Two-electrode voltage-clamp and electrophysiological studies

Isolated Malpighian tubules lying on the bottom of the perfusion bath were approximately 3.5 mm long. Since the open end of the tubule lumen is continuous with the electrical ground in the peritubular bath, concerns about short-circuiting transepithelial and membrane voltages were minimized by selecting principal cells approximately 0.5 mm from the blind end of the tubule, i.e. approx. 10 length constants away from the open end of the tubule (Aneshansley et al., 1988). We used piezo-electric remote control drives (PCS-5000; Burleigh Instruments Inc., Fishers, NY, USA) to impale the principal cell with both current and voltage electrodes (Fig. 1C). Impalements near the center of the cell yielded the most stable current and voltage records, some lasting as long as 3 h.

Conventional current and voltage microelectrodes (Kwik-Fil, Borosilicate Glass Capillaries, TW 100F-4; World Precision Instruments, Sarasota, FL, USA) were prepared as follows. After washing the glass capillaries with sulfuric–chromic acid cleaning solution and rinsing with distilled water, the capillaries were stored in a drying oven at 170°C until use. Capillaries were pulled on a programmable horizontal puller (Model P-87; Sutter Instruments, Novato, CA, USA) to yield resistances of 20–30 MΩ when filled with 3 mol l^{-1} KCl. Each principal cell was impaled with two electrodes, a voltage electrode for measurement of the basolateral membrane voltage (V_{bl}), and a current electrode for measurement of the input resistance, R_{pc} (Fig. 1C). Ag/AgCl wires connected the microelectrodes to the clamp circuit. The Ag/AgCl wire serving as ground in the peritubular Ringer solution was shielded with a 4% agar-Ringer bridge.

For most of the time, the impaled principal cell was left in the open-circuit condition, i.e. the cell was not voltage-clamped. The voltage-clamp circuit was engaged only when measurements of input resistance (R_{pc}) were of interest. We used the GeneClamp Model 500 Voltage and Patch Clamp Amplifier (Axon Instruments, Foster City, CA, USA), head stage HS-2A-×1LU for continuous measurements of the basolateral membrane voltage (V_{bl}) and the head stage HS-2A-×10MGU for current injection. R_{pc} was determined from steady currents in response to five progressive 10 mV hyperpolarizing voltage clamp steps of 11 ms duration, beginning at –20 mV on the hyperpolarizing side and ending at +20 mV on the depolarizing side of the basolateral membrane voltage (V_{bl}). Current–voltage (*I–V*) plots of the data were drawn using the program Clampfit (pClamp 6; Axon Instruments, Foster City, CA, USA). The plots yielded the input conductance, g_{pc}, as the slope of the best linear fit to the *I–V* plot. R_{pc} was determined as the inverse of g_{pc}. Current and voltage data were displayed on an oscilloscope (Iwatsu, Japan) and a strip chart recorder (model BD64; Kipp and Zonen, Crown Graphic). In addition we acquired and stored the data using the following hard- and software: a Macintosh computer (7300/200), Multifunction I/O Board PCI-1200, Signal Conditioning and Termination Board Model SC-2071, and LabView program version 4.1 (National Instruments Manufacturer, Austin, TX, USA).

Dose–response curves and measures of EC_{50}

The effect of each concentration of DNP or CN on the basolateral membrane voltage (V_{bl}) and cell input resistance (R_{pc}) was measured at least six times. The dose–response data were analyzed by the Hall, 4 parameter Regression of SigmaPlot (SPSS Science, Chicago, IL, USA) to yield values and standard errors of the EC_{50}.

Circuit analysis

In order to explain the analysis of data obtained by the methods of two-electrode voltage-clamp (TEVC) of a single principal cell of the tubule, it is useful to review the model of transepithelial NaCl and KCl secretion across the *Aedes aegypti* Malpighian tubule (Fig. 1A). The model circuit was originally derived from studies of isolated perfused Malpighian tubules (Beyenbach, 1995, 2001; Beyenbach and Petzel, 1987; Pannabecker et al., 1993; Yu and Beyenbach, 2001). Under control conditions the isolated *Aedes* Malpighian tubule secretes an approximately equimolar solution of NaCl and KCl (Fig. 1A). The cations Na^+ and K^+ take a transcellular pathway that passes through principal cells. The 'accompanying' anion, Cl^-, takes a shunt pathway located outside principal cells, apparently the paracellular pathway. The active transport pathway for Na^+ and K^+ through principal cells consists of electromotive forces (E) and resistances (R) at the basolateral (bl) and apical (a) membranes, respectively (Fig. 1B). The passive transport pathway for Cl^- consists of the shunt resistance (R_{sh}) alone. Active and passive transport pathways are parallel to each other, forming an intraepithelial current loop, such that cationic current through principal cells equals anionic current through the shunt. It follows that Cl^- is the 'accompanying' counterion for both Na^+ and K^+ secreted into the tubule lumen, which was confirmed experimentally by observing that rates of transepithelial Na^+ and K^+ secretion approximate the rate of transepithelial Cl^- secretion (Williams and Beyenbach, 1983, 1984). Transepithelial diffusion potentials are negligible for Na^+ and K^+ because the shunt pathway is virtually impermeable to these two major cations secreted into the tubule lumen (Williams and Beyenbach, 1984). Instead, the shunt pathway is permeable to Cl^-. However, transepithelial Cl^- diffusion potentials do not develop because the Cl^- concentration in the tubule lumen (161 mmol l^{-1}, Williams and Beyenbach, 1983) is similar to that in the peritubular Ringer (159 mmol l^{-1}). For these reasons, the shunt pathway R_{sh} has no transepithelial diffusion potential (E_{sh}) in the equivalent electrical circuit of the tubule (Fig. 1D).

In TEVC studies of a single principal cell (Fig. 1C), the resistance measured *via* intracellular electrodes is the input resistance (R_{pc}) of the cell, i.e. the resistance of the basolateral membrane in parallel to the resistances of the apical membrane and the shunt as shown in Fig. 1D:

$$R_{pc} = \frac{R_{bl}(R_a + R_{sh})}{R_{bl} + R_a + R_{sh}} . \quad (1)$$

The basolateral membrane voltage is:

$$V_{bl} = \left(\frac{E_{bl} + E_a}{R_{bl} + R_a + R_{sh}} \right) R_{bl} + E_{bl} . \quad (2)$$

The ratio V_{bl}/R_{pc} yields a current directly proportional to the electromotive forces and inversely proportional to the resistances of transport pathways:

$$\frac{V_{bl}}{R_{pc}} = \frac{E_a + 2E_{bl}}{R_a + R_{sh}} + \frac{E_{bl}}{R_{bl}} . \quad (3)$$

The meaning of this current becomes apparent by simplifying Equation 3. Previous studies have shown that under control conditions the electromotive force at the apical membrane (E_a=146.1 mV) is 8.35 times greater than the electromotive force at the basolateral membrane (E_{bl}=17.5 mV), and that the resistances of the basolateral membrane and the shunt are 2.114 and 1.474 times greater than the resistance of the apical membrane, respectively (Pannabecker et al., 1992; see also Fig. 1). Accordingly, Equation 3 can be reduced to reveal a current emanating from the apical membrane where the V-type H^+-ATPase is located:

$$\frac{V_{bl}}{R_{pc}} = \frac{0.56E_a}{R_a} = I_{at(virt)} . \quad (4)$$

The magnitude of the current depends largely on the electromotive force of the apical membrane and the resistance of the apical membrane (Fig. 1). If it is assumed that the electromotive force of the apical membrane E_a reflects largely the electromotive force of the V-type H^+-ATPase, and the R_a is the resistance of the apical membrane, including the internal resistance of the proton pump, then the ratio V_{bl}/R_{pc} approximates the active transport current (I_{at}) across the apical membrane, generated largely by the V-type H^+-ATPase. It is a virtual current because it is calculated and not measured. How close $I_{at(virt)}$ comes to the real current generated by the V-type H^+-ATPase depends on how close the electromotive force of the whole apical membrane (E_a) comes to the electromotive force of the V-type H^+-ATPase and how close R_a approaches the internal resistance of the V-type H^+-ATPase.

Statistical analysis

Most experiments were suitable for analysis by the Student's *t*-test for paired samples where each principal cell served as its own control. When this was not possible we consulted the *t*-test for unequal sample size and unequal variance. EC_{50} values were considered not significantly different if 3 S.E.M. of one EC_{50} included the mean of the other EC_{50}. Data are summarized as mean ± S.E.M. (N, number of observations).

Results

Dose–response curves of the effects of cyanide on basolateral membrane voltage and cell input resistance

After impaling a principal cell of the Malpighian tubule with current and voltage microelectrodes, we measured the basolateral membrane voltage (V_{bl}) with both electrodes. If the

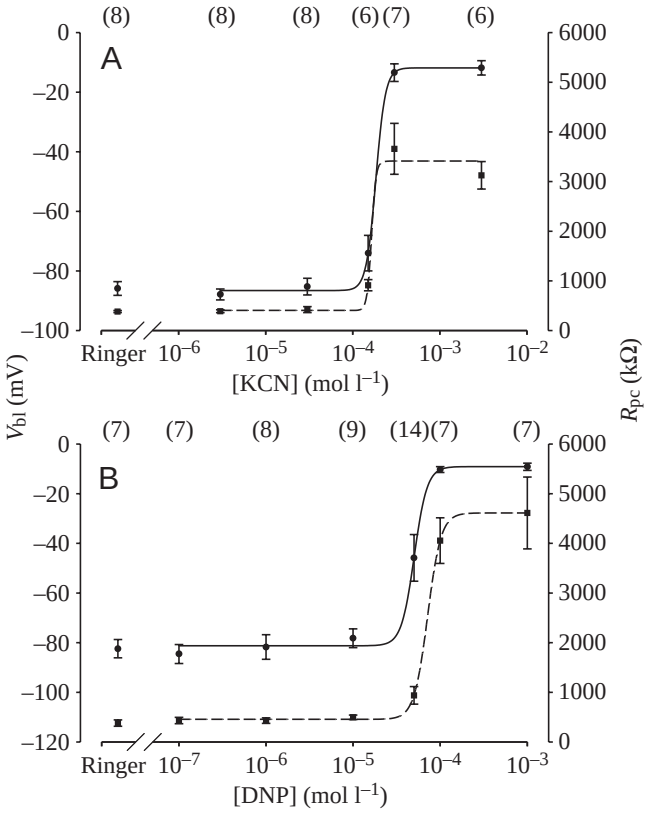

Fig. 2. Dose–response curves of the effects of (A) cyanide (KCN) and (B) dinitrophenol (DNP) on the basolateral membrane voltage (V_{bl}, solid line) and the input resistance (R_{pc}, broken line) of principal cells of Malpighian tubules of the yellow fever mosquito *Aedes aegypti*. EC_{50} is the concentration at half-maximum response. Values from 6–14 principal cells (in parentheses) are shown.

two voltage measurements were within 7% of each other, the experiment was continued. Values of V_{bl} were recorded continuously *via* the voltage electrode, and current was injected into the principal cell *via* the current electrode when measurements of the cell input resistance (R_{pc}) were of interest. After a control period of 5–20 min, the bath flow was switched to a Ringer solution containing one of five CN concentrations. V_{bl} was allowed to reach a new steady state, usually taking 2–10 min, when R_{pc} was measured again. The bath flow was then switched to control Ringer solution. After V_{bl} and R_{pc} had returned to within 4% of control values, the effect of another CN concentration was evaluated.

Plots of the peritubular CN concentration *versus* V_{bl} and R_{pc} yielded remarkably similar dose–response curves (Fig. 2A). CN had no effect on voltage or resistance at concentrations less than 100 μmol l^{-1} but a nearly complete effect at 300 μmol l^{-1}. Both dose–response curves were steep, with an EC_{50} of 184.0±22.3 μmol l^{-1} for the decrease in voltage and 164.4±3075 μmol l^{-1} for the increase in resistance. The two EC_{50} values were not significantly different. Steep dose–response curves usually result from cooperative interactions of reaction sites, but the evaluation of Hill coefficients is inappropriate here in view of the multiple steps in the cascade between the inhibition of ATP synthesis and its effect on voltage and resistance.

Dose–response curves of the effects of dinitrophenol on basolateral membrane voltage and cell input resistance

Plots of the peritubular DNP concentration *versus* V_{bl} and R_{pc} were also strikingly similar. DNP had no effect on voltage and resistance at concentrations less than 10 μmol l^{-1}, but a nearly complete effect at 100 μmol l^{-1} (Fig. 2B). Again, the dose–response curves were steep with an EC_{50} of 50.3±3.6 μmol l^{-1} for the decrease in voltage and 71.7±7.7 μmol l^{-1} for the increase in resistance. Again, the two EC_{50} values were not significantly different.

Effect of cyanide on intracellular ATP concentration, voltage and resistance of principal cells

Fig. 3 illustrates the temporal relationship between $[ATP]_i$ and the electrophysiological variables in Malpighian tubules, first under control conditions, then in the presence of cyanide, and finally upon washout. Since $[ATP]_i$ was measured in many Malpighian tubules these data are summarized as mean ± S.E.M. The electrophysiological data corresponding in time are from a single representative principal cell of a Malpighian tubule.

In freshly isolated Malpighian tubules, the control $[ATP]_i$ was 0.91±0.14 mmol l^{-1} in 16 determinations of five tubules each (90 Malpighian tubules in total). Control values of V_{bl}, R_{pc} and $I_{at(virt)}$ in the representative principal cell were –76 mV, 334 kΩ and 227.5 nA, respectively. The addition of cyanide to Malpighian tubules caused $[ATP]_i$ to plummet to 0.26±0.07 mmol l^{-1} within 15 s (11 sets of five Malpighian tubules; $P<0.0005$). $[ATP]_i$ measured 30 s after CN addition rose insignificantly to 0.32±0.09 mmol l^{-1} (11 sets of five Malpighian tubules) and then fell to 0.081±0.03 mmol l^{-1} at 2 min (5 sets of five Malpighian tubules). $[ATP]_i$ remained near this low value for the remaining time in cyanide.

The electrophysiological effects of CN lagged behind the effects on $[ATP]_i$. By the time $[ATP]_i$ had already decreased by 91% to 0.08 mmol l^{-1} (2 min in cyanide), V_{bl} had decreased only by 6.6% to –71 mV, with only a slight increase in R_{pc} from 334.1 to 439.5 kΩ. $I_{at(virt)}$ had decreased only 29.0% to 161.6 nA. After 3 min in the presence of CN, V_{bl} began to accelerate its depolarization to 0 mV, and R_{pc} began to rise in parallel while $I_{at(virt)}$ continued to decrease. Shortly before wash-out of CN, when $[ATP]_i$ was 0.11±0.03 mmol l^{-1} (after 8 min in cyanide), V_{bl} had reached a steady state of –8 mV, R_{pc} had climbed to 3150.8 kΩ, and $I_{at(virt)}$ had decreased to values close to zero (Fig. 3).

The effects of CN on V_{bl}, R_{pc} and $I_{at(virt)}$ clearly lagged behind the effects on $[ATP]_i$. Upon washout of CN, the reverse was observed as the recovery of $[ATP]_i$ lagged behind the recovery of electrophysiological variables. 2 min after washout of CN, V_{bl} had already returned to control values (Fig. 3). At the same time the input resistance had dropped 80.4%, from 3150.8 kΩ in cyanide to 616.9 kΩ, and $I_{at(virt)}$ had returned to 57.7% of control

values. However, $[ATP]_i$ remained near the low levels measured in the presence of CN. When V_{bl}, R_{pc} and $I_{at(virt)}$ had fully returned to control values approximately 12 min after washout, $[ATP]_i$ was just beginning to recover. It would take another 5 min for $[ATP]_i$ to approach control, pre-cyanide values.

The electrical responses to CN shown in Fig. 3 for a single representative principal cell were observed in seven additional principal cells where the effects of CN were investigated. The addition of 0.3 mmol l^{-1} KCN to the peritubular bath significantly (P<0.0001) depolarized V_{bl} from –85.9±2.5 mV (8 principal cells) to –13.4±3.2 mV (7), increased R_{pc} significantly (P<0.001) from 383.4±22.5 kΩ (8) to 3659.9±554.9 kΩ (7), and significantly (P<0.0001) decreased $I_{at(virt)}$ from 229.0±8.5 nA (8) to 4.2±0.15 nA (7). The electrophysiological effects of CN were observed 7–12 min after addition to the bath, with a mean time of approximately 9 min.

Effects of dinitrophenol on intracellular ATP concentrations and the conductance of basolateral and apical membranes of principal cells

Metabolic inhibition of the tubules with DNP yielded effects similar to those of KCN. $[ATP]_i$ significantly (P<0.02) fell from 0.91±0.27 mmol l^{-1} (9 principal cells) to 0.088±0.05 mmol l^{-1} 2 min after adding DNP. Approximately 3 min later, V_{bl} significantly (P<0.0001) depolarized from –82.4±4.0 mV (7) to –10.3±1.3 mV (7), R_{pc} significantly (P<0.001) rose from 381.3±69.3 kΩ (7) to 4055.5±495.9 kΩ (7), and $I_{at(virt)}$ significantly (P<0.001) decreased from 250.4±11.4 nA (7) to 2.6±0.3 nA (7). The effects of DNP on electrophysiological variables confirm previous observations (Beyenbach and Masia, 2002; Masia et al., 2000).

The effect of metabolic inhibition on the basolateral membrane K^+-conductance of principal cells

In view of the marked increase in the cell input resistance during metabolic inhibition, we explored the effects of CN on the K^+-conductance of the basolateral membrane of principal cells. The K^+-conductance was of interest because it is the dominant ionic conductance of that membrane in principal cells of *Aedes aegypti* (Beyenbach, 2001; Beyenbach and Masia, 2002; Masia et al., 2000).

Fig. 4 summarizes observations made in five principal cells where the response of the basolateral membrane to brief tenfold increases in the peritubular K^+ concentration was evaluated first in the absence and then in the presence of 0.3 mmol l^{-1} KCN. Control values in this series of experiments were V_{bl} –80.0±4.1 mV and R_{pc} was 495.3±61.8 kΩ. When the peritubular $[K^+]$ was increased from 3.4 mmol l^{-1} to 34 mmol l^{-1}, V_{bl} significantly (P<0.05) depolarized to –50.2±4.9 mV. In parallel, R_{pc} significantly (P<0.05) decreased to 434.9±50.1 kΩ. These effects were fully reversible upon restoring the control K^+ concentration.

Upon changing the peritubular Ringer solution to include 0.3 mmol l^{-1} CN, V_{bl} significantly (P<0.0002) decreased to –0.4±2.8 mV while R_{pc} significantly (P<0.05) increased to 1378.4±282.9 kΩ. In the presence of CN, the basolateral membrane voltage failed to respond to the tenfold increase in peritubular K^+ concentration (Fig. 4). Likewise, R_{pc} was not affected by the increase in peritubular K^+ concentration.

The loss of the basolateral membrane K^+-conductance in the presence of CN was confirmed with barium (Fig. 5). Barium is known to block K^+-channels in principal cells of the *Aedes* Malpighian tubule (Masia et al., 2000). In the present study, the addition of 5 mmol l^{-1} Ba^{2+} to the peritubular bath

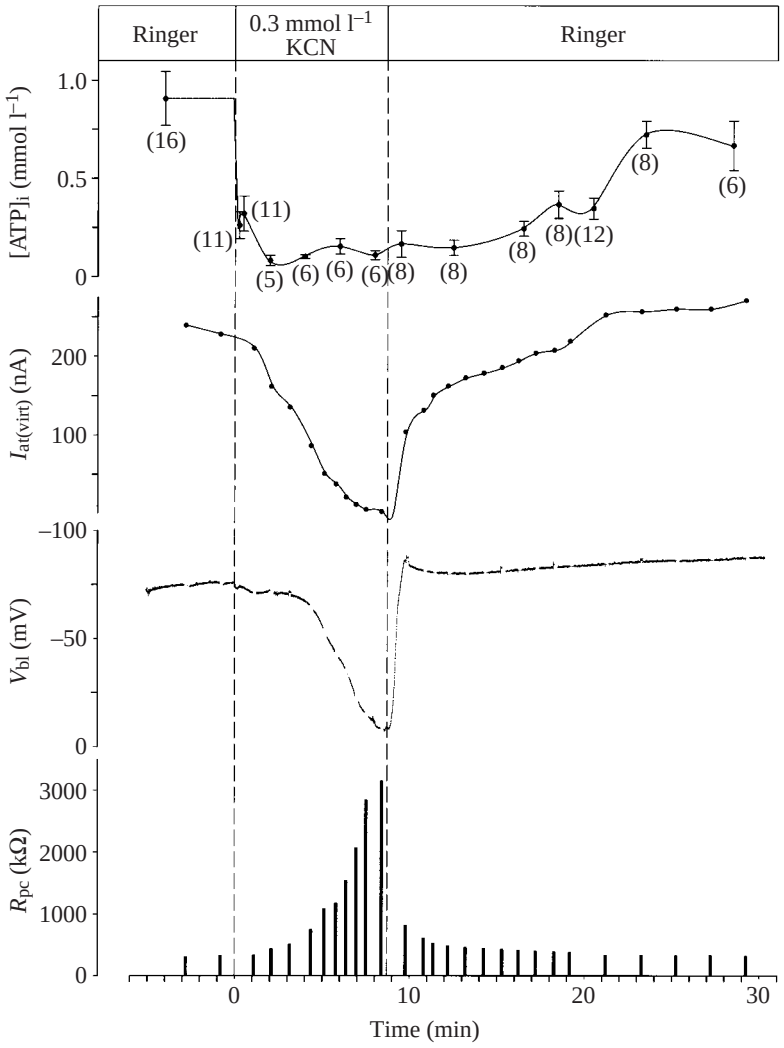

Fig. 3. Time course of the effects of 0.3 mmol l^{-1} cyanide (KCN) on the basolateral membrane voltage (V_{bl}), input resistance (R_{pc}), and the virtual active transport current ($I_{at(virt)}$) in a representative principal cell, and on intracellular ATP concentrations $[ATP]_i$ in 6–16 sets of five Malpighian tubules each. Values are mean ± S.E.M. (number of tubule sets). The temporal relationship between the electrical variables and [ATP] are approximate because exchanging the peritubular medium to include CN took 43 s in the electrical assay and 10 s in the ATP assay.

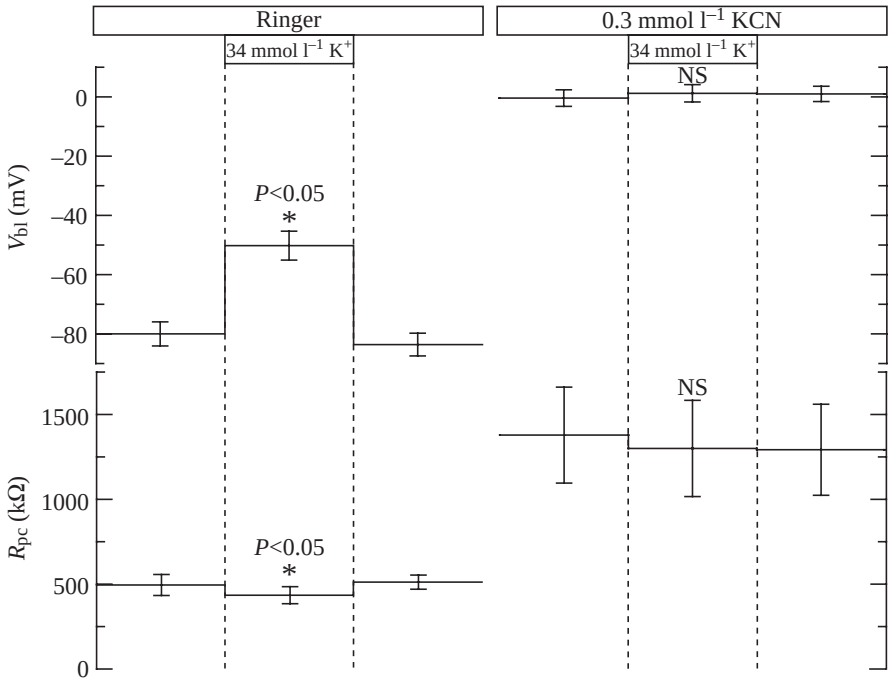

Fig. 4. Loss of the K^+-conductance of the basolateral membrane of principal cells after metabolic inhibition with CN. K^+-conductance was evaluated by the effects of a tenfold increase in bath [K^+], from 3.4 mmol l^{-1} to 34 mmol l^{-1}, on the basolateral membrane voltage V_{bl} and input resistance R_{pc} of principal cells of Malpighian tubules isolated from *Aedes aegypti*. Values are means ± S.E.M. of five cells. NS, not significant.

significantly (P<0.0001) hyperpolarized V_{bl} from –79.5±2.2 mV (50) to –89.1±3.1 mV (50), and significantly (P<0.0001) increased R_{pc} from 488.9±32.3 kΩ (50) to 769.4±40.2 kΩ (50). These effects were reversible upon Ba^{2+} washout. When Ba^{2+} was added to the peritubular bath in the presence of 0.3 mmol l^{-1} CN, there were no effects on V_{bl} and R_{pc}, indicating that K^+-channels had already closed (Fig. 5).

Discussion

ATP and electrogenic and electroconductive transport mechanisms

We first tend to think of ATP as fuel of active transport pumps and other energy requiring processes that rely on the hydrolysis of ATP. In addition to its role as an energy source, ATP, or the ATP/ADP ratio, can serve as a regulator of pumps, carriers and channels. In the present study we have observed evidence for both energizing and regulatory roles of ATP. The inhibition of ATP synthesis by cyanide or dinitrophenol withheld ATP from the V-type H^+-ATPase at the apical membrane, thereby stalling the principal energizer of transepithelial transport across the Malpighian tubule (Beyenbach, 2001). As a result, the voltage across the apical membrane depolarized and with it the voltage across the basolateral membrane, because the two membranes are electrically coupled through the shunt pathway, R_{sh} (Fig. 1B). In addition to inhibiting the V-type H^+-ATPase, the inhibition of ATP synthesis led to the closure of K^+-channels at the basolateral membrane.

ATP synthesis was inhibited in two distinct steps of oxidative phosphorylation: cyanide was used to prevent the generation of proton gradients across the inner mitochondrial membrane, and dinitrophenol was used to collapse it. By inhibiting cytochrome oxidase complexes, cyanide inhibits the formation of proton gradients that are needed to drive

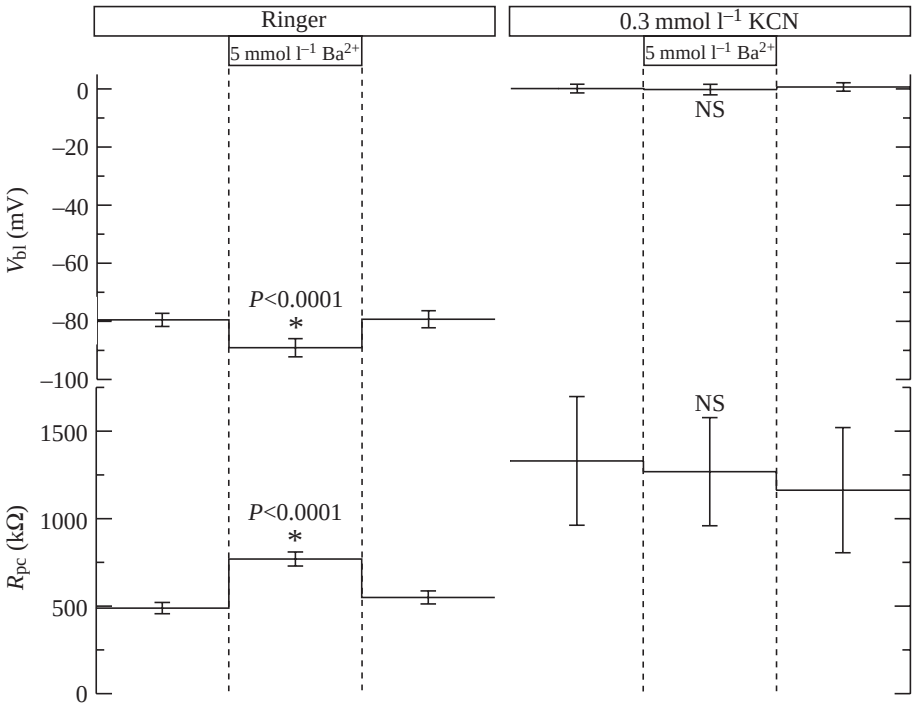

Fig. 5. Loss of Ba^{2+}-blockade of K^+-channels of the basolateral membrane of principal cells after metabolic inhibition with CN. The effect of peritubular $BaCl_2$ (5 mmol l^{-1}), a competitive blocker of K^+-channels, was evaluated on basolateral membrane voltage V_{bl} and input resistance R_{pc} of principal cells of Malpighian tubules isolated from *Aedes aegypti*. Values are means ± S.E.M. of 9–50 cells. NS, not significant.

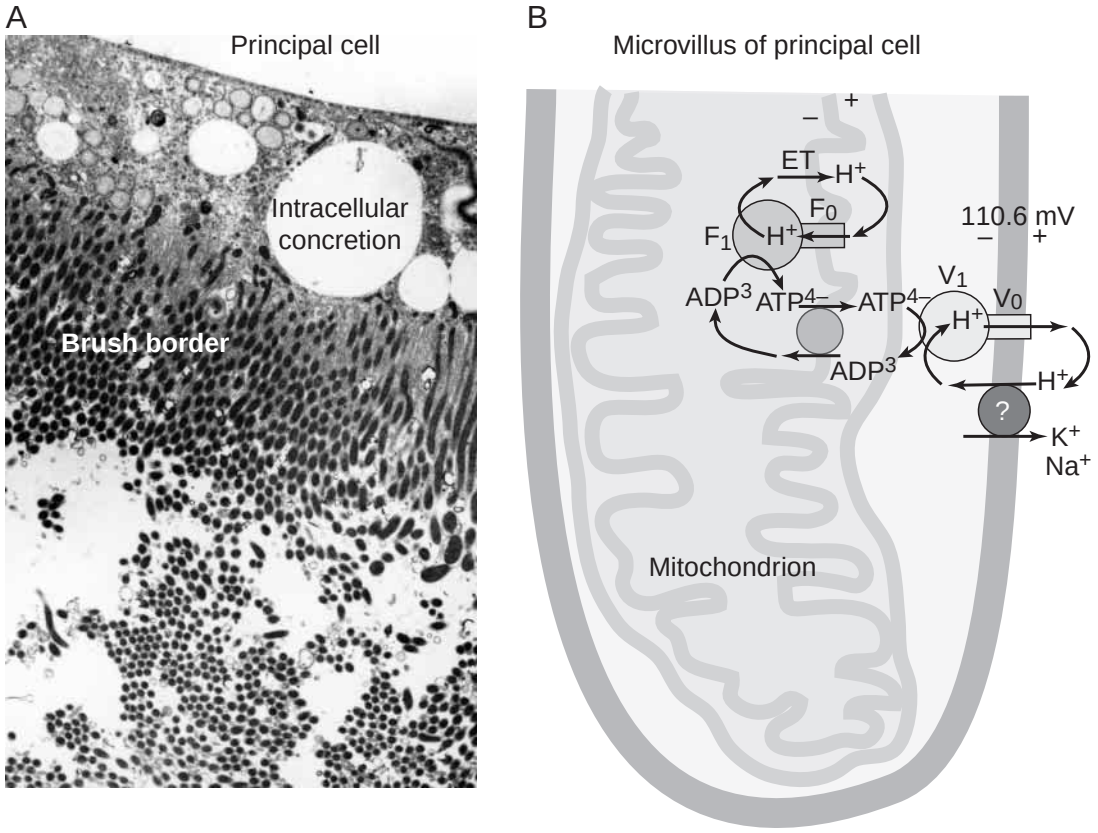

Fig. 6. The apical brush border membrane of principal cells in Malpighian tubules of *Aedes aegypti*. The apical membrane is characterized by a tall, mitochondrion-rich brush border (A) which brings the site of ATP synthesis in close proximity to the site of utilization (B). ATP is synthesized at the inner mitochondrial membrane by the ATP synthase, consisting of the catalytic F_1 segment and the proton-conducting F_0 segment. What drives ATP synthesis is the proton gradient generated by the electron transport chain (ETC). ATP^{4-} is transported across the inner membrane in exchange for ADP^{3-}. ATP^{4-} goes on to diffuse across the outer mitochondrial membrane to the apical membrane of the brush border. The hydrolysis of ATP by the V-type H^+-ATPase powers H^+ transport into the micro-environment of the brush border, thereby generating a large apical membrane voltage (–110.6 mV on average). The H^+ electrochemical potential thus established across the apical membrane can drive the extrusion of Na^+ and K^+ *via* nH^+/cation exchange transporter(s) that have yet to be isolated.

synthases, the enzymes of ATP synthesis. In addition, cyanide may also inhibit glycolysis by binding to NAD^+, thereby preventing its reduction to NADH. Cyanide caused $[ATP]_i$ to drop to values below 9% of control levels and to reduce transepithelial electrolyte secretion to less than 2%, as judged from the drop of the virtual active transport current $I_{at(virt)}$ from 229.0 nA to 4.2 nA.

In contrast to cyanide, DNP allows the electron transport chain to continue, but proton gradients across the inner mitochondrial membrane cannot develop because of the H^+-leak pathway provided by DNP. DNP is lipid soluble. Sequestered in lipid membranes including the inner mitochondrial membrane, DNP functions like a H^+-carrier (H^+-ionophore). The inward proton flux bypasses ATP synthases, thereby averting the formation of ATP. DNP caused $[ATP]_i$ to drop to values less than 10% of control, and it reduced transepithelial transport to 1% of control in view of the drop of the virtual active transport current $I_{at(virt)}$ from 250.4 nA to 2.6 nA. Though the mechanisms of action of cyanide and DNP differ, their convergence by affecting V_{bl}, R_{pc} and $I_{at(virt)}$ in similar ways points to the requirement of ATP for the maintenance of electrogenic and conductive transport pathways.

Coupling of intracellular ATP to transepithelial transport

The inhibition of ATP synthesis by famine or toxin should be devastating for a cell. However, neither cyanide nor DNP reduced $[ATP]_i$ to zero. Instead, $[ATP]_i$ dropped to levels 10% of control in the presence of CN or DNP and remained at this new steady state concentration. The nearly complete inhibition of $I_{at(virt)}$, to 2% and 1% of control in the presence of cyanide and DNP, respectively, suggests that $[ATP]_i$ has fallen below threshold concentrations of the V-type H^+-ATPase, thereby preventing the further hydrolysis of ATP. For this reason $[ATP]_i$ may not have fallen below 10% of control concentrations.

Next to inhibiting the V-type H^+-ATPase at the apical membrane, metabolic inhibition caused the cell input

resistance R_{pc} to increase fivefold or more, reflecting in part the loss of K^+-conductance at the basolateral membrane (Figs 3–5). Thus, the inhibition of ATP synthesis affected transport steps at opposite poles of the cell, suggesting a physiological control mechanism: when K^+ exit across the apical membrane into the tubule lumen cannot be energized by the V-type H^+-ATPase deprived of ATP, K^+ entry into the cell across the basolateral membrane is blocked. The inhibition of both pump and channels effectively isolates the cell from epithelial transport loads, thereby maintaining intracellular homeostasis. When the environment for oxidative phosphorylation improves again, the cell can mount a quick recovery with little energy input. Indeed, upon washout of cyanide or DNP, which restored ATP synthesis, the recovery of V_{bl}, R_{pc} and open K^+-channels was swift, needing only a minute or two (Fig. 3).

What was observed in the present study at the all-or-none extremes of oxidative phosphorylation may take place within the normal physiological range of $[ATP]_i$, coupling available energy to rates of transepithelial transport. ATP may mediate this regulation directly and/or indirectly *via* changes in intracellular pH, Ca^{2+} concentrations and other signaling pathways.

Inhibition of the V-type H⁺-ATPase

Cyanide and DNP reduced $[ATP]_i$ to values of 80–90 μmol l^{-1}, in the vicinity of the K_m for ATP of V-type H^+-ATPases. The K_m of V-type H^+-ATPase in the midgut of the tobacco hornworm *Manduca sexta* is 250 μmol l^{-1} for ATP (Schweikl et al., 1989). If the K_m is similar in the *Aedes aegypti* Malpighian tubule, then the pump activity would drop to 26% of control rates when the $[ATP]_i$ drops to 90 μmol l^{-1} in the presence of DNP or CN. Since the virtual active transport current dropped to 1%, there must be additional mechanisms for inhibiting the V-type H^+-ATPase. Inhibition of the proton pump by ADP comes first to mind. ADP is known to inhibit V-type H^+-ATPases (Brauer and Tu, 1994; Simon and Burckhardt, 1990). As ADP concentrations go up, or ATP/ADP ratios go down, during metabolic inhibition, the catalytic cytosolic V_1 sector of the V-type H^+-ATPases dissociates from the transmembrane V_0 sector that now no longer conducts H^+ ions (Kane and Parra, 2000). The dissociation can be induced in yeast cells by depriving them of glucose, and reversed by supplying the sugar again, suggesting that assembly and disassembly of the holoenzyme is a general physiological mechanism that regulates V-type H^+-ATPases (Kane and Parra, 2000; Merzendorfer et al., 1997). A second way that cyanide and DNP may inhibit the V-type H^+-ATPase is *via* redox modulation (Harvey and Wieczorek, 1997). V-type H^+-ATPases require reducing conditions for activity. In contrast, oxidizing conditions inhibit the proton pump, apparently by facilitating the formation of disulfide bonds in the catalytic V_1 sector that prevent ATP from binding (Feng and Forgac, 1994). Harvey and Wieczorek have suggested that mitochondria, often in close proximity to the V-type H^+-ATPase, may produce the reducing conditions suitable for pump activity (Harvey and Wieczorek, 1997; Merzendorfer et al., 1997).

Mechanisms that increase the input resistance of the cell

The similarity of the EC_{50} values for the effect of cyanide on voltage and resistance is striking (Fig. 2A). Likewise, the EC_{50} values for the effect of DNP on voltage and resistance are surprisingly alike (Fig. 2B). Similar EC_{50} values for the effects on voltage and resistance suggest a single target, such as the V-type H^+-ATPase, where the withdrawal of ATP from the pump affects both electrogenic and conductive properties of the proton pump. Withholding ATP from the proton pump is expected to reduce the electromotive force of V-type H^+-ATPase, thereby reducing the apical membrane voltage as well as the basolateral membrane voltage *via* coupling through the shunt (Masia et al., 2000). In parallel, the separation of the V_1 sector from the holoenzyme leaves a non-conducting V_0 sector in the apical membrane that is expected to increase the resistance of the apical membrane and with it, the input resistance of the cell. Thus, concomitant effects on voltage and resistance yielding similar EC_{50} values could largely stem from effects of metabolic inhibition on the V-type H^+-ATPase located at the apical membrane. However, K^+-diffusion potentials across the basolateral membrane (Fig. 4), and the effects of barium in the absence and presence of KCN (Fig. 5) illustrate that metabolic inhibition also affects the resistance of the basolateral membrane. In particular, K^+-channels in the basolateral membrane close during metabolic inhibition, thereby contributing to the increase in cell input resistance (Figs 3–5). The mechanism that causes basolateral membrane K^+-channels to shut down is subject to speculation. ATP, Ca^{2+} and Mg^{2+} concentrations, pH, membrane voltage and phosphorylation are all known to affect the activity of K^+-channels (Hille, 2001). ATP-regulated K^+-channels (K_{ATP}) open when $[ATP]_i$ is low, which is opposite to the closing we observe in the present study (Figs 4, 5). Voltage-dependent regulation is another possibility, but most K^+-channels open at depolarization of the membrane voltage (Hille, 2001), whereas in the present study depolarization of the basolateral membrane voltage was associated with channel closure. On the other hand, depolarizing membrane voltages are known to drive intracellular Mg^{2+} ions into the pore of open K^+-channels, thereby blocking them (Lee et al., 1999). Additional studies are needed to characterize the type of K^+-channels inhabiting the basolateral membrane of principal cells and to learn their mechanisms of regulation.

In addition to resistance changes at apical and basolateral membranes of principal cells, the closing of gap junctions between principal cells may contribute to the increase in input resistance during metabolic inhibition. In a previous study we have estimated that on average 5–6 principal cells are electrically coupled (Masia et al., 2000). ATP depletion is associated with the uncoupling of gap junctions in ischemic cardiac cells, which is apparently mediated *via* elevated cytosolic Ca^{2+} concentration (Dekker et al., 1996). Further experiments are necessary to elucidate the contribution of gap

junctions to the measurements of input resistance in single principal cells of the *Aedes* Malpighian tubules.

Kinetics of metabolic and electrophysiological events

$[ATP]_i$ dropped rapidly during metabolic inhibition (Fig. 3). It took only 15 s for $[ATP]_i$ to fall by 73% upon addition of cyanide to the peritubular medium. Technical limits of the method did not allow us to measure ATP at times earlier than 15 s. Thus, metabolic rates might be even higher than those indicated by the available data.

In view of the close proximity of the sites of ATP synthesis (mitochondria) and electrogenesis (ATP-dependent V-type H^+-ATPase) in the brush border of principal cells (Fig. 6), we expected $[ATP]_i$ and electrical variables to change in parallel, without a time lag, upon the addition of cyanide. However, in the experiment, $[ATP]_i$ consistently dropped in advance of the effects on voltage, resistance and virtual active transport current (Fig. 3). For example, it took only 2 min for the average whole cell ATP concentration to drop to 10% of control values after the addition of cyanide to the peritubular medium, but nearly 6 min for the virtual active transport current to decrease by the same percentage (Fig. 3). Although some delay (33 s) can be attributed to differences in experimental protocol (see legend to Fig. 3), most of the delay, more than 5 min for $I_{at(virt)}$ to drop to 10% of control, appears to have a physiological basis. As a first hypothesis, cytosolic ATP in the vicinity of the brush border can continue to fuel the V-type H^+-ATPase for some time when mitochondrial ATP synthesis is blocked. Intracellular diffusion of ATP can also explain why $I_{at(virt)}$ recovers well in advance of cytosolic ATP concentration upon washout of cyanide (Fig. 3). In this case, the first ATP generated by mitochondria in the brush border serves to fuel V-type H^+-ATPases close by. Additional ATP can then move on and increase cytosolic ATP concentrations in the cell.

Entry of K^+ from the hemolymph into the cell

Wherever the electrophysiological properties of basolateral membranes have been studied in Malpighian tubules, a prominent K^+-conductance has been found, whether the tubule secretes or reabsorbs K^+ (Beyenbach and Masia, 2002; Haley and O'Donnell, 1997; Neufeld and Leader, 1998; Nicolson and Isaacson, 1990; Weltens et al., 1992; Wessing et al., 1993). Blocking the K^+-conductance with Ba^{2+} or rubidium suggests the presence of K^+-channels, but their type have yet to be identified in any Malpighian tubule (Haley and O'Donnell, 1997; Hyde et al., 2001; Leyssens et al., 1994; Wessing et al., 1993). The addition of Ba^{2+} to the peritubular medium of the tubule leads to the hyperpolarization of basolateral membrane voltage, together with an increase in membrane resistance, consistent with the hypothesis that pump current returning to the cytoplasmic face of the V-type H^+-ATPase is carried by K^+ across the basolateral membrane (Beyenbach, 2001; Masia et al., 2000). Supporting the model of the electrophoretic entry of K^+ from the hemolymph into the epithelial cell is the distribution of intracellular K^+ at or near electrochemical equilibrium with extracellular K^+ in Malpighian tubules of ants and the alpine weta (Neufeld and Leader, 1998). However, K^+-channels are not the exclusive entry pathway for K^+. Other transport mechanisms mediating K^+ entry may include the Na^+/K^+ ATPase (Anstee et al., 1986; Grieco and Lopes, 1997; Linton and O'Donnell, 1999; Xu and Marshall, 1999) and possibly KCl and Na/K/2Cl cotransport systems (Leyssens et al., 1994).

Aw and Jones (1985) have hypothesized that, similar to cytosolic ATP gradients, pH gradients may exist in the cytosol, especially in cells with active proton pumps such as the V-type H^+-ATPase. Indeed, the inhibition of the V-type H^+-ATPase with bafilomycin led to intracellular acidification in Malpighian tubules of *Drosophila* (Wessing et al., 1993), and metabolic inhibition of Malpighian tubules in the ant also acidified the cytoplasm (Leyssens et al., 1993). Thus, K^+-channels in basolateral membranes of Malpighian tubules may be pH-sensitive, closing at intracellular acidification. Consistent with this hypothesis is the finding that epithelial K^+-channels reduce their activity at intracellular acidification (Harvey, 1995; McNicholas et al., 1998; Onken et al., 1990).

Midgut goblet cells in Manduca sexta *and principal cells in* Aedes aegypti *Malpighian tubules*

The observations of the effects of metabolic inhibition we made in principal cells of the *Aedes aegypti* Malpighian tubule are remarkably similar to those made in epithelial goblet cells of the lepidopteran midgut (Zeiske et al., 2002). To begin, both the *Aedes* principal cell and the *Manduca* goblet cell secrete K^+ from hemolymph to lumen (or goblet cavity) *via* active, electrogenic transport processes. The entry of K^+ from the hemolymph into both cells is mediated *via* Ba^{2+}-blockable K^+-channels, driven by current returning to the cytoplasmic face of the V-type H^+-ATPase (Zeiske et al., 1986). The extrusion of K^+ across the apical membrane of the goblet cell is thought to be mediated by an electrogenic $K^+/2H^+$ transporter that in turn is driven by the H^+ electrochemical potential set up by the V-type H^+-ATPase across the apical membrane (Azuma et al., 1995). In essence, the model of transepithelial K^+ secretion in goblet cells does not differ from the present, widely accepted model of K^+ secretion across Malpighian tubules.

Metabolic inhibition of goblet cells with azide led to the immediate inhibition of the short-circuit current, documenting the inhibition of transepithelial K^+ secretion when the V-type H^+-ATPase at the apical membrane is deprived of ATP. In parallel, the K^+ permeability of the basolateral membrane decreased (Zeiske et al., 2002). Thus, metabolic inhibition inhibits epithelial transport steps at both apical and basolateral membranes, not only in principal cells of *Aedes* Malpighian tubules but also in goblet cells of *Manduca* midgut. These striking similarities support the hypothesis expressed above that ATP integrates transport steps at basolateral and apical membranes of epithelial cells. However, the study of Zeiske et al., went on to show that intracellular acidification duplicated the effects of metabolic inhibition on (1) apical membrane 'K^+ pump' currents, and (2) on basolateral membrane K^+ permeability in the *Manduca*

midgut (Zeiske et al., 2002). The effect of intracellular acidification on $[ATP]_i$ was not measured in goblet cells. Hence it remains to be seen whether intracellular pH, independently of ATP, can integrate transport steps at the apical and basolateral cell membranes.

The authors gratefully acknowledge undergraduate fellowships from the Howard Hughes Foundation and the American Physiological Society awarded to D.S.W. and NSF grants IBN 9604394 and 0078058 awarded to K.W.B. We thank Helmut Wieczorek (University of Osnabrück, Germany) and Peter C. Hinkle (Ithaca, NY, USA) for fruitful discussions and Bruce Schultz (Kansas State University, USA) for assistance with the data analysis.

References

Aneshansley, D. J., Marler, C. E. and Beyenbach, K. W. (1988). Transepithelial voltage measurements in isolated Malpighian tubules of *Aedes aegypti*. *J. Insect Physiol.* **35**, 41-52.

Anstee, J. H., Baldrick, P. and Bowler, K. (1986). Studies on ouabain-binding to (Na^++K^+)-ATPase from Malpighian tubules of the locust, *Locusta migratoria* L. *Biochim. Biophys. Acta* **860**, 15-24.

Aw, T. Y. and Jones, D. P. (1985). ATP concentration gradients in cytosol of liver cells during hypoxia. *Am. J. Physiol.* **249**, C385-392.

Azuma, M., Harvey, W. R. and Wieczorek, H. (1995). Stoichiometry of K^+/H^+ antiport helps to explain extracellular pH 11 in a model epithelium. *FEBS Lett.* **361**, 153-156.

Beyenbach, K. W. (1995). Mechanism and regulation of electrolyte transport in Malpighian tubules. *J. Insect Physiol.* **41**, 197-207.

Beyenbach, K. W. (2001). Energizing epithelial transport with the vacuolar H^+-ATPase. *News Physiol. Sci.* **16**, 145-151.

Beyenbach, K. W. and Masia, R. (2002). Membrane conductances of principal cells in Malpighian tubules of *Aedes aegypti*. *J. Insect Physiol.* **48**, 375-386.

Beyenbach, K. W. and Petzel, D. H. (1987). Diuresis in mosquitoes: Role of a natriuretic factor. *News Physiol. Sci.* **2**, 171-175.

Brauer, D. and Tu, S. I. (1994). Effects of ATP analogs on the proton pumping by the vacuolar H^+-ATPase from maize roots. *Physiol. Plant.* **91**, 442-448.

Dekker, L. R., Fiolet, J. W., VanBavel, E., Coronel, R., Opthof, T., Spaan, J. A. and Janse, M. J. (1996). Intracellular Ca^{2+}, intracellular electrical coupling, and mechanical activity in ischemic rabbit papillary muscle. *Circ. Res.* **79**, 237-246.

Feng, Y. and Forgac, M. (1994). Inhibition of vacuolar H^+-ATPase by disulfide bond formation between cysteine 254 and cysteine 532 in subunit A. *J. Biol. Chem.* **269**, 13224-13230.

Grieco, M. A. B. and Lopes, A. G. (1997). 5-hydroxytryptamine regulates the Na^+/K^+-ATPase activity in Malpighian tubules of *Rhodnius prolixus*: Evidence for involvement of G-protein and cAMP-dependent protein kinase. *Arch. Insect Biochem. Physiol.* **36**, 203-214.

Haley, C. A. and O'Donnell, M. J. (1997). K^+ reabsorption by the lower Malpighian tubule of *Rhodnius prolixus*: Inhibition by Ba^{2+} and blockers of H^+/K^+-ATPases. *J. Exp. Biol.* **200**, 139-147.

Harvey, B. J. (1995). Cross-talk between sodium and potassium channels in tight epithelia. *Kidney Int.* **48**, 1191-1199.

Harvey, W. R. and Wieczorek, H. (1997). Animal plasma membrane energization by chemiosmotic H^+ V-ATPases. *J. Exp. Biol.* **200**, 203-216.

Hille, B. (2001). *Ion Channels of Excitable Membranes*. Sunderland: Sinauer Associates, Inc.

Hyde, D., Baldrick, P., Marshall, S. L. and Anstee, J. H. (2001). Rubidium reduces potassium permeability and fluid secretion in Malpighian tubules of *Locusta migratoria*, L. *J. Insect Physiol.* **47**, 629-637.

Kane, P. M. and Parra, K. J. (2000). Assembly and regulation of the yeast vacuolar H^+-ATPase. *J. Exp. Biol.* **203**, 81-87.

Lee, J. K., John, S. A. and Weiss, J. N. (1999). Novel gating mechanism of polyamine block in the strong inward rectifier K channel Kir2.1. *J. Gen. Physiol.* **113**, 555-564.

Leyssens, A., Dijkstra, S., Van Kerkhove, E. and Steels, P. (1994). Mechanisms of K^+ uptake across the basal membrane of Malpighian tubules of *Formica polyctena*: The effect of ions and inhibitors. *J. Exp. Biol.* **195**, 123-145.

Leyssens, A., Zhang, S.-L., Van Kerkhove, E. and Steels, P. (1993). Both dinitrophenol and Ba^{2+} reduce KCl and fluid secretion in Malpighian tubules of *Formica*: The role of the apical H^+ and K^+ concentration gradient. *J. Insect Physiol.* **39**, 1061-1073.

Linton, S. M. and O'Donnell, M. J. (1999). Contributions of K^+:Cl^- cotransport and Na^+/K^+-ATPase to basolateral ion transport in Malpighian tubules of *Drosophila melanogaster*. *J. Exp. Biol.* **202**, 1561-1570.

Masia, R., Aneshansley, D., Nagel, W., Nachman, R. J. and Beyenbach, K. W. (2000). Voltage clamping single cells in intact Malpighian tubules of mosquitoes. *Am. J. Physiol.* **279**, F747-F754.

McNicholas, C. M., MacGregor, G. G., Islas, L. D., Yang, Y., Hebert, S. C. and Giebisch, G. (1998). pH-dependent modulation of the cloned renal K^+ channel, ROMK. *Am. J. Physiol.* **275**, F972-F981.

Merzendorfer, H., Graf, R., Huss, M., Harvey, W. R. and Wieczorek, H. (1997). Regulation of proton-translocating V-ATPases. *J. Exp. Biol.* **200**, 225-235.

Neufeld, D. S. and Leader, J. P. (1998). Electrochemical characteristics of ion secretion in Malpighian tubules of the New Zealand alpine weta (*Hemideina maori*). *J. Insect Physiol.* **44**, 39-48.

Nicolson, S. and Isaacson, L. (1990). Patch clamp of the basal membrane of beetle Malpighian tubules: Direct demonstration of potassium channels. *J. Insect Physiol.* **36**, 877-884.

Onken, H., Zeiske, W. and Harvey, B. (1990). Effect of mucosal H^+ and chemical modification on transcellular K^+ current in frog skin. *Biochim. Biophys. Acta* **1024**, 95-102.

Pannabecker, T. L., Aneshansley, D. J. and Beyenbach, K. W. (1992). Unique electrophysiological effects of dinitrophenol in Malpighian tubules. *Am. J. Physiol.* **263**, R609-R614.

Pannabecker, T. L., Hayes, T. K. and Beyenbach, K. W. (1993). Regulation of epithelial shunt conductance by the peptide leucokinin. *J. Membr. Biol.* **132**, 63-76.

Schweikl, H., Klein, U., Schindlbeck, M. and Wieczorek, H. (1989). A vacuolar-type ATPase, partially purified from potassium transporting plasma membranes of tobacco hornworm midgut. *J. Biol. Chem.* **264**, 11136-11142.

Simon, B. J. and Burckhardt, G. (1990). Characterization of inside-out oriented H^+-ATPases in cholate-pretreated renal brush-border membrane vesicles. *J. Membr. Biol.* **117**, 141-151.

Weltens, R., Leyssens, A., Zhang, S. L., Lohrmann, E., Steels, P. and Van Kerkhove, E. (1992). Unmasking of the apical electrogenic proton pump in isolated Malpighian tubules (*Formica polyctena*) by the use of barium. *Cell. Physiol. Biochem.* **2**, 101-116.

Wessing, A., Bertram, G. and Zierold, K. (1993). Effects of bafilomycin A1 and amiloride on the apical potassium and proton gradients in *Drosophila* Malpighian tubules studied by X-ray microanalysis and microelectrode measurements. *J. Comp. Physiol. B* **163**, 452-462.

Williams, J. C. and Beyenbach, K. W. (1983). Differential effects of secretagogues on Na and K secretion in the Malpighian tubules of *Aedes aegypti* (L.). *J. Comp. Physiol.* **149**, 511-517.

Williams, J. C. and Beyenbach, K. W. (1984). Differential effects of secretagogues on the electrophysiology of the Malpighian tubules of the yellow fever mosquito. *J. Comp. Physiol. B* **154**, 301-309.

Xu, W. and Marshall, A. T. (1999). X-ray microanalysis of the Malpighian tubules of the black field cricket *Teleogryllus oceanicus*: The roles of Na K ATPase and the Na K 2Cl cotransporter. *J. Insect Physiol.* **45**, 885-893.

Yu, M. J. and Beyenbach, K. W. (2001). Leucokinin and the modulation of the shunt pathway in Malpighian tubules. *J. Insect Physiol.* **47**, 263-276.

Zeiske, W., Meyer, H. and Wieczorek, H. (2002). Insect midgut K^+ secretion: Concerted run-down of apical/basolateral transporters with extra-/intracellular acidity. *J. Exp. Biol.* **205**, 463-474.

Zeiske, W., Van Driessche, W. and Ziegler, R. (1986). Current-noise analysis of the basolateral route of K^+ ions across a K^+-secreting insect midgut epithelium (*Manduca sexta*). *Pfluegers Arch.* **407**, 657-663.